Industrial Crops & Products 246 (2026) 123224

Contents lists available at ScienceDirect

Industrial Crops & Products

journal homepage: www.elsevier.com/locate/indcrop

Integrative mechanisms of Mn peroxidase-dominated fungal digestion and CaO depolymerization for synergistic enhancement of biomass saccharification towards distinct bioethanol and lactic acid conversions in desired *Miscanthus*

Jiamin Li [a,1], Yixiang Wang [a,b,1], Yasi Zhou [a], Siqin Tan [a], Jiale Liu [a], Qian Zhang [a], Ruilan Yang [a], Hao Peng [c], Peng Liu [a], Yanting Wang [a], Liangcai Peng [a,b], Heng Kang [a,2,*]

[a] *Key Laboratory of Fermentation Engineering (Ministry of Education), National "111" Center for Cellular Regulation & Molecular Pharmaceutics, Cooperative Innovation Center of Industrial Fermentation (Ministry of Education & Hubei Province), Hubei Key Laboratory of Industrial Microbiology, Biomass & Bioenergy Research Centre, School of Life & Health Sciences, Hubei University of Technology, Wuhan 430068, China*

[b] *College of Plant Science & Technology, Huazhong Agricultural University, Wuhan 430070, China*

[c] *Shandong Provincial Key Laboratory of Energy Genetics, CAS Key Laboratory of Biofuels, Qingdao Institute of Bioenergy & Bioprocess Technology, Chinese Academy of Sciences, Shandong Energy Institute, Qingdao New Energy Shandong Laboratory, Qingdao 266101, China*

ARTICLE INFO

Keywords:
Miscanthus straw
White-rot fungi
Bioethanol
Lactic acid
Enzymatic saccharification
Proteomics
Metabolomics

ABSTRACT

Crop straws represent the enormous biomass resources convertible for sustainable biofuels and valuable biochemicals, but lignocellulose recalcitrance basically necessitates highly-efficient biomass processes under green-like manner. By incubating desirable *Miscanthus* (Msa6) straw with two classic white-rot fungi strains, this study examined effective wall polymer extractions from fungal secretions of four major types of lignocellulose-degradation enzymes and cofactors along with distinct metabolisms. Notably, the *Lentinula edodes* incubation secreted manganese peroxidase at extremely high activity for dominating lignin-network deconstruction, whereas the *Pleurotus ostreatus* incubation produced laccase with high activity for contribution to polysaccharide depolymerization indirectly through lignin oxidation and synergistic action with hydrolytic enzymes. Furthermore, the integrative *L. edodes* and CaO pretreatments could mostly cause lignocellulose depolymerization accountable for much raised biomass porosity such as the specific surface area and pore volume raised by 47% and 44%, which resulted in a synergistically enhanced biomass enzymatic saccharification for the highest hexose yield raised by 33%, compared to the control (optimal CaO pretreatment with raw straw). Meanwhile, despite of relatively less hexose yield obtained, the integrated *P. ostreatus* and CaO pretreatments achieved the higher bioethanol and lactic acid yields than those of the controls by 40% and 41%, probably due to releasing the less toxic compounds that inhibit yeast and bacterial fermentations. Based on all major findings achieved, this study finally proposes a novel mechanism model to elucidate why synergistic lignocellulose depolymerization and modification are achieved from integration of two green-like pretreatments, thereby offering a selective strategy for enhancing hexoses, bioethanol and lactic acid productivity in bioenergy crops.

1. Introduction

Lignocellulose is the most abundant renewable resource on the earth, offering considerable production of sustainable biofuels and valuable biochemicals (Paz Cedeno et al., 2025). Lignocellulose is primarily composed of cellulose, hemicellulose, and lignin, which together form a complex matrix that constitutes structural framework of plant cell walls (Wang et al., 2024). However, intrinsic lignocellulose recalcitrance, mainly arising from the tightly interlinked lignin–carbohydrate network, causes a low-efficient biomass enzymatic saccharification and

* Corresponding author.
E-mail address: hkang@mail.hzau.edu.cn (H. Kang).
[1] Equal contributor
[2] Web: http://bbrc.hbut.edu.cn.

https://doi.org/10.1016/j.indcrop.2026.123224
Received 26 December 2025; Received in revised form 23 March 2026; Accepted 6 April 2026

high-costly biofuel conversion (Meenakshisundaram et al., 2021; Wan and Li. 2012).

To reduce lignocellulose recalcitrance, conventional acid and alkali pretreatments have been broadly implemented with diverse lignocellulose substrates by co-extraction of hemicellulose and lignin, but they basically require extreme conditions such as high temperatures and high concentrations, leading to the secondary waste release. (Beluhan et al., 2023; Zhang et al., 2023a). These challenges have stimulated interests in green-like pretreatments by using recyclable chemicals and green liquors or inoculating fungal penetration, and white-rot fungi treatments are considered as particularly promising solution due to their unique enzymatic repertoire and selective lignin-degrading capacity (Chen and Davaritouchaee. 2023; Saha et al., 2016).

White-rot fungi produce a diverse repertoire of extracellular oxidative enzymes such as manganese peroxidase (MnP), lignin peroxidase (LiP) and laccase (Lac), which oxidatively cleave lignin polymers with minimal cellulose degradation for improving cellulose accessibility (Civzele et al., 2023; Kipping et al., 2024). This selectivity is attributed to their ability to attack both phenolic and non-phenolic lignin units through radical-mediated reactions, preserving carbohydrate integrity for subsequent biomass saccharification (Deswal et al., 2014; Nguyen et al., 2024; Qi et al., 2023). For instance, *Irpex lacteus* achieves 43.8% lignin degradation in corn stover under non-sterile conditions, resulting in a sevenfold increase in enzymatic hydrolysis efficiency (Song et al., 2013). Similarly, sequential treatments using *Ganoderma lobatum* and *Gloeophyllum trabeum* have demonstrated synergistic delignification for significantly enhancing glucose yields from wheat straw (Hermosilla et al., 2018). Despite these advantages, fungal pretreatment is constrained by limitations such as extended incubation periods, variability in strain–substrate specificity, and potential holocellulose loss (Ding et al., 2019). To overcome those limitations, integrated biological and chemical pretreatments are being employed, but it remains to explore advanced technology for efficient biomass procsses with zero-biomass release.

Miscanthus is a leading bioenergy crop worldwide, due to its fast growth and well adaptation to environmental stress (Fan et al., 2024). The diverse *Miscanthus* accessions could not only provide enormous biomass resources, but they also represent distinct lignocelluloses recalcitrance (Alam et al., 2019; Brischke and Hanske. 2016; da Costa et al., 2019). In this study, we selected two representative *Miscanthus* accessions (Msa56, Msa6) distinctive at lignocellulose compositions and wall polymer features accountable for different lignocellulose recalcitrance (Fig. S1) (Ai et al., 2024). By performing time-course incubations with three types of mushroom fungal strains, this study determined distinctive lignocellulose depolymerization, and the optimal selectivity index was identified from desired Msa6 incubation with two fungi *(Pleurotus ostreatus* and *Lentinula edodes*) by calculation of lignin degradation ratio against cellulose degradation ratio. The fungal de-lignocellulose was further pretreated with mild CaO for reducing lignocellulose recalcitrance, leading to a synergistic enhancement of biomass enzymatic saccharification. Furthermore, this study performed yeast and *L. paracasei* fermentations for distinct bioethanol and lactic acid conversions, and all remaining residues were re-utilized for fungal growth as edible food source as described. Notably, based on proteomic assay and metabolomics profiling, this study finally proposed a novel mechanism model about how fungi involve in lignocellulose depolymerization, providing an integrative strategy applicable for efficient biomass enzymatic saccharification towards distinct biofuel and biochemical conversions under a green manner.

2. Material and methods

2.1. Biomass and fungal strains preparation

Miscanthus straws were harvested from the experimental fields of Huazhong Agricultural University (Wuhan, China) during the 2023–2024 growing season. Two genotypes (Msa56 and Msa6) were selected based on their distinct lignocellulose composition. Stems were oven-dried at 60 °C to a constant weight, mechanically ground, and sieved through a 40-mesh screen (425 μm) to obtain uniform powders. The powdered biomass was stored in a sealed container at room temperature until in use. The white-rot fungal strains (*Ganoderma lucidum*, *Pleurotus ostreatus*, and *Lentinula edodes*) obtained from the Biomass and Bioenergy Research Laboratory, Hubei University of Technology, were maintained on potato dextrose agar (PDA) slants at 4 °C and subcultured monthly. Active mycelia from 7-day-old PDA plates were used for incubation with *Miscanthus* lignocellulose as biological pretreatment.

2.2. Fungal pretreatment of Miscanthus lignocellulose

Biological pretreatment of *Miscanthus* was conducted using a solid-state fungal cultivation method in 250 mL glass culture bottles. Each bottle was loaded with 10 g of *Miscanthus* powder and 30 mL of mineral nutrient solution (2 g/L KH_2PO_4, 0.5 g/L $MgSO_4{\cdot}7H_2O$, 0.1 g/L $CaCl_2$, and 10 mg/L thiamine; pH 6.0). The mixtures were thoroughly homogenized and sterilized by autoclaving at 121 °C for 30 min. Six PDA plugs (1 cm in diameter) with full fungal mycelia were aseptically inoculated into the sterilized lignocellulose substrates, and incubated at 28 °C under static dark for 28 days as previously described (de Cassia Spacki et al., 2023). Samples were respectively collected under time-course incubation (7, 14, 21, and 28 days) after fungal material was carefully removed using a sterile spatula (Ding et al., 2019). The residual substrate was separated by filtration through sterile gauze, and the filtrate was centrifuged at 6000 *g* for 10 min at 4 °C to collect the supernatant for enzyme activity assay. Crude enzyme extracts were obtained by re-suspending the mycelial mats in citrate buffer (pH 4.8) for laccase and manganese peroxidase activity assay *in vitro*. The insoluble residual biomass was washed three times with distilled water and dried to a constant weight at 60 °C. Control treatments were subjected to the same sterilization and incubation procedures without fungal inoculation. All experiments were accomplished at independent triplicate.

2.3. Chemical (CaO) pretreatment and enzymatic hydrolysis

A series of CaO pretreatments were conducted under different CaO concentrations (0%, 5%, 10%, 15%, 20%, and 25% w/w), reaction temperature (60, 80, and 100 °C), and reaction time (0, 3, 6, and 9 h) (Li et al., 2024). After the samples were centrifuged at 6000 *g* for 10 min, the lignocellulose residues were employed for enzymatic hydrolysis using 0.16% (w/v) the mixed-cellulases (cellulases at 10.60 FPU/g biomass and xylanase at 6.72 U/g biomass) obtained from Imperial Jade Biotechnology Co., Ltd. (HSB, Ningxia 750002, China). The enzymatic hydrolysis was conducted in a total reaction volume of 6 mL containing 0.3 g pretreated lignocellulosic substrate, corresponding to a solid loading of 5% (w/v). The reaction mixture was prepared in citrate buffer (pH 4.8), supplemented with 1% (v/v) Tween-80 and conducted at 50 °C with shaking at 150 rpm for 48 h. After centrifugation, the supernatants were collected for sugars yield assay as previously described (Li et al., 2018). Total hexoses (as glucose equivalents) and pentoses (as xylose equivalents) were respectively determined by the anthrone/H_2SO_4 orcinol/HCl methods (Baksi et al., 2019). All assays were performed under independent triplicate.

2.4. Bioethanol and lactic acid fermentations

For ethanol fermentation, the enzymatic hydrolysate was sterilized and incubated with our engineered yeast strain (E4, He et al., 2022) statically at 37 °C for 48 h. For lactic acid fermentation, the sterilized hydrolysate supernatant was adjusted to pH 5.5 and incubated with *Lactobacillus paracasei* (provided by the Fermentation Engineering Laboratory, College of Life Science and Technology, Huazhong Agricultural

University) at 37 °C for 36 h. After fermentations, the supernatants were respectively collected for measurements of ethanol and lactic acid concentrations as previously described (Cheng et al., 2019; Liu et al., 2024). All experiments were accomplished under independent triplicate.

2.5. Enzyme activity assay

The crude enzyme extracts were collected from fungal incubation with *Miscanthus* lignocellulose, and were prepared following the extraction procedure described in Section 2.2. The activities of manganese peroxidase (MnP) and laccase (Lac) were respectively determined *in vitro* using commercial assay kits (Boxbio, Beijing, China) according to the manufacturer's instructions (Hu et al., 2021). All experiments were performed in independent triplicate.

2.6. Proteomics analysis

Proteomic analyses of crude enzyme extracts were conducted by LC-MS/MS (Pu Ao Biotechnology Co., Ltd., Wuhan, China; Orbitrap Elite LC-MS/MS, Thermo, USA). The gel bands of target proteins were cut into small pieces (approximate1 mm x 1 mm), treated with destaining solution for 5 min, and washed three times. The gel pieces were then incubated with washing buffer at 26 °C with shaking at 1000 rpm for 30 min, dehydrated with pure acetonitrile for 5 min, and dried under air. Reduction was performed by adding a reducing solution at 50 °C for 30 min, followed by washing with ammonium bicarbonate and subsequent alkylation at 25 °C in the dark for 40 min. The gel pieces were further washed thoroughly with washing buffer and ammonium bicarbonate, dehydrated again with acetonitrile, and dried. Proteins were digested overnight at 37 °C by adding trypsin solution to cover the gel pieces. Peptides were extracted twice with extraction solution, and the combined supernatants were collected for subsequent mass spectrometry analysis. The samples were sequentially washed with acetonitrile and 0.1% formic acid by centrifugation twice to remove impurities. The sample solution was collected by centrifugation and washed again with 0.1% formic acid. Desalting columns were transferred to new tubes and eluted with 60% acetonitrile containing 0.1% formic acid. The eluates were collected, lyophilized, and dissolved in 0.1% formic acid for further analysis. Samples were analysed using a Thermo Easy-nLC 1000 liquid chromatography system coupled to a Q Exactive HF-X mass spectrometer. Peptides were separated on a C18 reversed-phase column (1.8 μm, 0.15 × 100 mm) with 0.1% formic acid in water and 100% acetonitrile as mobile phases at a flow rate of 600 nL/min over a 98-min gradient. Protein identification and quantification were accomplished using MaxQuant 2.1 software and the databases from Uniprot for *Lentinus edodes* and *Pleurotus ostreatus* (uniprot-*Lentinus_edodes*.fasta; uniprot-*Pleurotus_ostreatus*. fasta).

2.7. Metabolomics analysis

Metabolites were profiled using a Waters ACQUITY I-Class PLUS UPLC system coupled with a Xevo G2-XS QTOF mass spectrometer (Waters, USA). Separation was accomplished on an ACQUITY UPLC HSS T3 column (1.8 μm, 2.1 × 100 mm) with 0.1% formic acid in water (A) and acetonitrile (B) as mobile phases. Data were acquired in MSE mode using MassLynx V4.2 with a high-energy range of 10–40 V. ESI conditions included capillary voltage 2500 V (positive) or −2000 V (negative), source temperature 100°C, and desolvation temperature 500°C. Raw data were processed in Progenesis QI for peak alignment and normalization, and metabolites were annotated using METLIN and in-house databases. Differential metabolites were identified based on | FC= > 1.5, $p < 0.05$, and VIP > 1, and pathway enrichment was conducted using KEGG.

2.8. Determination of soluble sugars and cell wall composition

Soluble sugars and polysaccharides were extracted and quantified as reviously described (Peng et al., 2000). Lignin content was determined using a modified two-step acid hydrolysis method (Li et al., 2018). The biomass power was firstly extracted with benzene-ethanol (2:1 v/v) for 4 h to remove extractives. The extracted residue was then hydrolyzed with 67% (v/v) H_2SO_4 at room temperature for 1.5 h, followed by dilution to 2.88% H_2SO_4 and incubation at 120 °C for 1 h. Acid-soluble lignin (ASL) in supernatant was measured by UV spectroscopy at 205 nm. The remaining solid residue was incinerated at 575 ± 25 °C for 4 h, and the acid-insoluble lignin (AIL) content was calculated from the weight loss after ash correction. Total lignin content was calculated as the sum of ASL and AIL (Li et al., 2024; Yu et al., 2025). All assays were accomplished under independent triplicat.

2.9. Physicochemical and structural characterization of residues

After the integrative pretreatments, the obtained solid residues were repeatedly washed with deionized water until neutral pH to remove residual chemical reagents and soluble by-products. The washed samples were then dried in a forced-air oven at 60 °C to constant weight. After drying, the samples were ground and sieved through a 60-mesh screen to obtain powders with uniform particle size. The lignocellulose samples were characterized by advanced technology including scanning electron microscopy (SEM, TESCAN MIRA LMS, Czech Republic), Fourier-transform infrared microspectroscopy (FTIR, Thermo Scientific, Nicolet iN10, USA), and X-ray diffraction (XRD, Lans Scientific, China). The specific surface area, pore size distribution, and pore volume of the biomass residues were evaluated by an automated surface area and porosity analyzer (BET, Micromeritics ASAP 2460, USA).

2.10. Reuse of enzymatic hydrolysis residues as fungal culture medium

The enzyme-undigestible residues of *Miscanthus* were collected, oven-dried at 60 °C to constant weight, and milled to pass through a 40-mesh sieve. *Pleurotus ostreatus* was inoculated onto either standard potato dextrose agar (PDA) or the solid media supplemented with enzyme-undigestible residues powders at 2%, 4%, and 6% (w/v). Cultures were incubated at 25 °C for 7 days under dark. Mycelial growth was assessed by harvesting the biomass, rinsing with distilled water, and oven-drying at 60 °C to constant weight for dry-weight determination.

2.11. Statistical calculation

The major experiments were conducted with three biological replicates (n = 3), and each replicate was originated from an independent cultivation or pretreatment batch. Technical replicates were performed for analytical measurements. Mean values and standard deviation (SD) were calculated using Microsoft Excel 2021 (Redmond, WA, USA). Graphical representations, including point diagrams with fitted curves and histograms, were generated using Origin 8.5 software (Microcal Software, Northampton, MA). One-way ANOVA was performed using SigmaPlot 11.2.0.5 to assess significant differences among treatments.

3. Results and discussion

3.1. Distinct depolymerization of Miscanthus accessions from fungal incubations

In this study, we selected two *Miscanthus* accessions (Msa56 and Msa6) distinctive at lignocellulosic compositions and wall polymer features (Tables S1 & S2). As a comparison, the Msa6 accession contained significantly less cellulose and lignin levels than those of Msa56 accession by 12% and 17%, leading to hemicellulose content raised by 39% at $p < 0.001$ level (n = 3). In terms of wall polymers features, the

Msa6 accession showed either reduced crystalline index or increased degree of polymerization of cellulose microfibrils, compared to the Msa56, whereas H- and S-monomer proportions of lignin substrates were significantly varied between two accessions (Li et al., 2014; Pei et al., 2016; Skiba et al., 2026; Yu et al., 2025). Using these two distinct *Miscanthus* accessions, this study initially performed biological pretreatments by incubating with three white-rot fungal species (*Ganoderma lucidum*, *Pleurotus ostreatus*, and *Lentinula edodes*; Fig. S2). Under time-course fungal incubations for 7 days to 28 days (Fig. S3), a consistently lignocellulose depolymerization was observed between two *Miscanthus* accessions (Table 1; Tables S3 & S4). As a comparison, the *L. edodes* incubation caused relatively more lignin and hemicellulose coextractions with less cellulose reduction among the three fungi incubations, whereas the *P. ostreatus* incubation showed slightly more lignin and hemicellulose coextractions than those of the *G. lucidum*. Meanwhile, the three fungi incubations with Msa6 accession were relatively more effective for lignin and hemicellulose coextractions, which should be accounting for its lower lignocellulose recalcitrance compared to the Msa56 (Derba-Maceluch et al., 2025). As a comprehensive comparison, the selectivity index (SI) values were evaluated among the three fungi incubations with two *Miscanthus* accessions (Table 2), and the SI calculated as the ratio of lignin degradation to cellulose degradation, is specifically accounting for the preferential lignin degradation by fungus rather than for the total extent of biomass degradation. As a result, the Msa56 accession achieved the highest SI values (1.3, 1.08) from 28-day incubation with *P. ostreatus* and *L. edodes* strains, respectively, but about 19% biomass was lost at this stage (Table S3). But, the Msa6 accession remained high SI values (1.12, 1.62) with relatively less biomass loss from 21-day incubations with *P. ostreatus* and *L. edodes* (Table S4). Even though the *G. lucidum* strain showed a high SI value from 28-day incubation with Msa6 accession, about 26% of total biomass was lost, which should not be considerable strain for biological pretreatment. Therefore, combined SI metrics with acceptable less biomass loss, the *P. ostreatus* and *L. edodes* were selected for further experiments in this study.

Table 2
Selectivity index (SI) of three fungi (*G. lucidum*, *P. ostreatus*, *L. edodes*) incubations with mature straws of two *Miscanthus* (Msa56, Msa6) accessions under time course.

Sample	Incubation days	Fungal strain		
		G. lucidum	*P. ostreatus*	*L. edodes*
Msa56	7	0.34 ± 0.08^{c}	1.84 ± 1.3^{a}	0.68 ± 0.17^{bc}
	14	0.46 ± 0.07^{c}	1.49 ± 0.31^{ab}	0.61 ± 0.1^{bc}
	21	0.67 ± 0.07^{bc}	0.68 ± 0.06^{bc}	0.91 ± 0.18^{bc}
	28	0.65 ± 0.08^{bc}	1.3 ± 0.18^{abc}	1.08 ± 0.18^{abc}
Msa6	7	0.2 ± 0.13^{e}	0.16 ± 0.14^{e}	0.54 ± 0.24^{de}
	14	0.66 ± 0.55^{de}	0.47 ± 0.29^{de}	1.93 ± 1.19^{bc}
	21	0.88 ± 0.31^{bcde}	1.12 ± 0.27^{bcde}	1.62 ± 0.3^{bcd}
	28	3.27 ± 1.18^{a}	0.72 ± 0.08^{cde}	2.1 ± 0.59^{ab}

SI was calculated as the ratio of lignin degradation to cellulose degradation, based on the absolute mass loss of lignin and cellulose; Data as means ± SD (n = 3) and small letters (a-d) as multiple *t*-test at $p < 0.05$ level among all data presented

3.2. Characteristic enzyme activity and proteomics profiling of fungal incubation

To understand lignocellulose depolymerization from fungal incubations, this study determined two major de-lignin enzymes activities from fungi incubations with two *Miscanthus* accessions *in vitro* (Fig. 1). As a result, the *P. ostreatus* and *L. edodes* strains showed much higher manganese peroxidase (MnP) activities than those of the *G. lucidum*, in particular after 14–21days incubations with desired Msa6 accession (Fig. 1 C), which confirmed their distinct de-lignin capacities as examined above. By comparison, the *P. ostreatus* strain remained higher laccase activity, whereas other fungi strains had relatively low ones after 14-day incubations (Fig. 1 B & D), indicating that the MnP enzyme could consistently play a major role for lignin depolymerization of *Miscanthus* lignocelluloses. To confirm this finding, proteomics assays were conducted for two major fungi (*P. ostreatus*, *L. edodes*) incubations with Msa6 accession (Tables 3 and 4), and the MnP enzyme was identified with much higher coverages than those of the laccase enzyme, being consistent with their distinct enzyme activities examined *in vitro*. Meanwhile, other three groups of the enzymes were identified for xylan and cellulose digestions and modifications, but the enzymes types and quantities of each group were varied between two fungal incubations, suggesting a distinct metabolism of for lignocellulose depolymerization (de Figueiredo et al., 2021; Li et al., 2023; Qi et al., 2025). Notably, as both fungi strains secreted a conserved set of oxidative and hydrolytic enzymes such as lytic polysaccharide monooxygenase (LPMO), carboxymuconolactone decarboxylase, β-glucosidase, and cellobiohydrolase, indicating a shared oxidative–hydrolytic framework for effective lignocellulose depolymerization (Monteiro et al., 2025; Pellegrino et al., 2022).

3.3. Diverse metabolomic pathways from fungal secretions

As two fungi incubations distinctively released the enzyme activities and enzyme compositions, this study conducted metabolomic assays of the supernatants released from two fungal incubations with the desired Msa6 accession (Fig. S4). In general, ten metabolism pathways were at least identified based on available data, but they were mostly different between two fungi incubations (Fig. 2; Fig. S5), indicating that multiple metabolisms were distinctively enriched in two fungi strains for secreting lignocellulose-degradation enzymes. Further combined with proteomics assays with higher abundances of multicopper oxidase, aryl-alcohol oxidase, glyoxal oxidase, and manganese peroxidase from *L. edodes* incubation, its metabolomic profiles exhibited consequent enrichment of oxidative and lipid-derived metabolites such as riboflavin, linoleic acid, and stearidonic acid together with activation of α-linolenic acid metabolism and monoterpenoid biosynthesis pathways (Huang et al., 2022; Tang et al., 2020). In this system, α-linolenic acid primarily acts as a redox mediator for directly participating in reactions

Table 1
Biomass composition (% dry matter) alterations of two *Miscanthus* (Msa56, Msa6) accessions after incubated with three fungi (*G. lucidum*, *P. ostreatus*, and *L. edodes*) for 21 days.

	Sample	Cellulose (%)	Hemicellulose (%)	Lignin (%)	Other (%)	Weight loss (%)
Msa56	**Control**	29.39 ± 1.12	11.3 ± 0.16	23.04 ± 1.59	36.27 ± 0.53	NA
	G. lucidum	21.7 ± 1.07	10.47 ± 0.49	19.08 ± 0.22	35.91 ± 0.88	12.83 ± 0.78
	P. ostreatus	21.92 ± 0.45	8.54 ± 0.18	19.03 ± 0.53	36.37 ± 0.26	14.13 ± 1.11
	L. edodes	23.41 ± 0.38	8.43 ± 0.11	18.79 ± 0.73	36.84 ± 0.61	12.53 ± 0.05
Msa6	**Control**	25.84 ± 1.19	15.69 ± 0.27	19.18 ± 0.44	38.96 ± 0.25	NA
	G. lucidum	23.85 ± 0.57	9.4 ± 0.56	18.07 ± 0.27	30.41 ± 0.81	18.27 ± 0.26
	P. ostreatus	23.32 ± 0.12	9.68 ± 0.37	17.19 ± 0.46	37.31 ± 0.25	12.5 ± 0.24
	L. edodes	23.83 ± 0.24	9.25 ± 0.55	16.84 ± 0.71	34.48 ± 1.01	15.6 ± 0.22

Data as means ± SD (n = 3); Control as raw straw of *Miscanthus* without fungi incubation; NA as not available data.

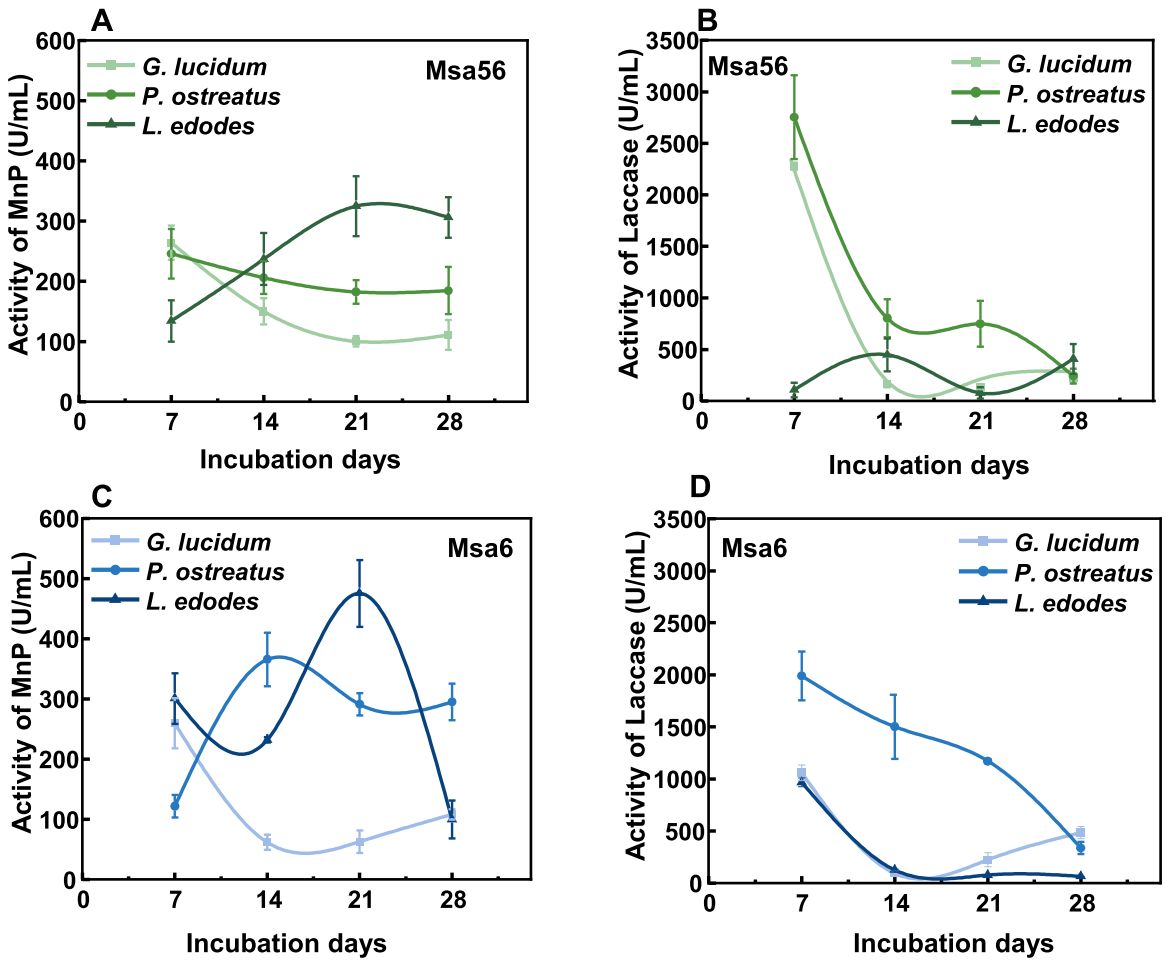

Fig. 1. Activity assays of manganese peroxidase (MnP) and laccase in the crude enzyme extracts of three fungi (*G. lucidum*, *P. ostreatus*, *L. edodes*) incubations with raw straws of two *Miscanthus* accessions (Msa56, Msa6) under time course. Data as means ± SD (n = 3).

Table 3
LC-MS/MS analysis of total enzymes secreted by *Pleurotus ostreatus* from 21-day incubation with Msa6 straw.

Enzyme type	Accession number	Coverage (%)	Peptides	Unique peptides
Manganese peroxidase	A0A1Q3DXT5	39	2	2
Laccase	A0A1Q3E7K8	8	1	1
endo-1,4-β-xylanase	A0A1Q3ENG9	10	5	5
1,4-β-xylosidase	A0A1Q3EF30	5	2	2
β-L-arabinofuranosidase	A0A1Q3DV08	6	1	1
Endoglucanase	A0A1Q3ET78	5	4	4
Cellobiohydrolase	A0A1Q3EU06	13	3	3
β-Glucosidase	A0A1Q3E9R7	6	2	2
Glyoxal oxidase	A0A1Q3ECK6	7	2	2
Carboxymuconolactone decarboxylase	A0A1Q3E9L4	5	1	1
	A0A1Q3E9T1	16	1	1
Lytic polysaccharide monooxygenase (LPMO)	A0A1Q3ECE1	19	4	4

Table 4
LC-MS/MS analysis of enzymes secreted by *Lentinula edodes* from 21-day incubation with pretreated Msa6 straw.

Enzyme type	Accession number	Coverage (%)	Peptides	Unique peptides
Manganese peroxidase	A0A8H6ZTD6	13	2	2
Laccase	B7XGB7	8	1	1
endo-1,4-β-xylanase	A0A8H7DNA7	3	2	2
1,4-β-xylosidase	A0A8H6ZHH2	2	1	1
Endoglucanase	A0A8H6ZVZ0	9	2	2
Cellobiohydrolase	A0A8H7DTU0	3	1	1
β-Glucosidase	A0A8H7A7N7	1	1	1
Glyoxal oxidase	A0A8H6ZID9	2	1	1
Aryl-alcohol oxidase	A0A8H7A1A0	1	1	1
Multicopper oxidase	A0A8H6ZYI6	2	2	2
Lytic polysaccharide monooxygenase (LPMO)	A0A8H6ZLZ7	7	3	3

from initiating and sustaining lipid peroxidation chain reactions to generating highly reactive oxidative species, which could destruct the recalcitrant structure of lignin (Kapich et al., 2010). In addition, white-rot fungi not only degrade lignocellulose but also produce diverse secondary metabolites, including terpenoids and phenolic compounds during their metabolic processes (Pinar and Rodríguez-Couto. 2024). This findings reveal a dominated deconstruction of the lignin network via radical-mediated oxidation, in which lipid peroxidation derivatives may act as mediators or secondary messengers in ligninolytic processes for improved wall polysaccharides accessibility (Zhao et al., 2024). In contrast, the *P. ostreatus* incubation showed relatively lower oxidative metabolites, but had potentially higher accumulation of carbohydrate derivatives, suggesting a metabolic strategy towards a direct hydrolytic depolymerization of hemicellulose and cellulose as supported by its distinct enzyme secretion profile (He et al., 2024; Pellegrino et al., 2022; Siaperas et al., 2025). This interpretation is supported by the previous studies about elevated hydrolytic enzyme activities during substrate colonization and composting such as cellulolytic enzymes

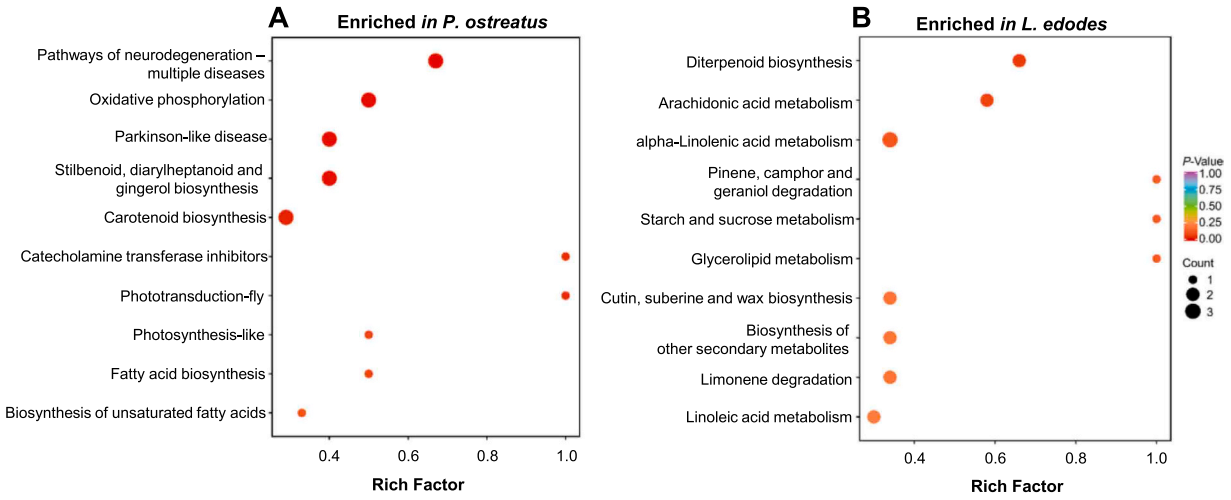

Fig. 2. KEGG pathway enrichment analyses of metabolomes from two fungal incubations with *Miscanthus* straws for 21 days. (A) *Pleurotus ostreatus*; (B) *Lentinula edodes*. Each bubble represents a specific KEGG pathway and the Rich Factor (x-axis) indicates the proportion of differentially enriched metabolites mapped to a given pathway; The bubble size corresponds to the number of metabolites within the pathway, and the color intensity represents the *p*-value from the enrichment analysis, with a darker color as greater statistical significance.

(endoglucanase, cellobiohydrolase, β-glucosidase) and hemicellulolytic enzymes (xylosidase, glucuronidase) (Hřebečková et al., 2020; Petraglia et al., 2025). Therefore, while *L. edodes* appears to rely mainly on strong oxidative metabolism to modify lignin and generate reactive intermediates, whereas *P. ostreatus* was likely to engage in hydrolytic cleavage of wall polysaccharides although this remains to be validated in the futural experiments.

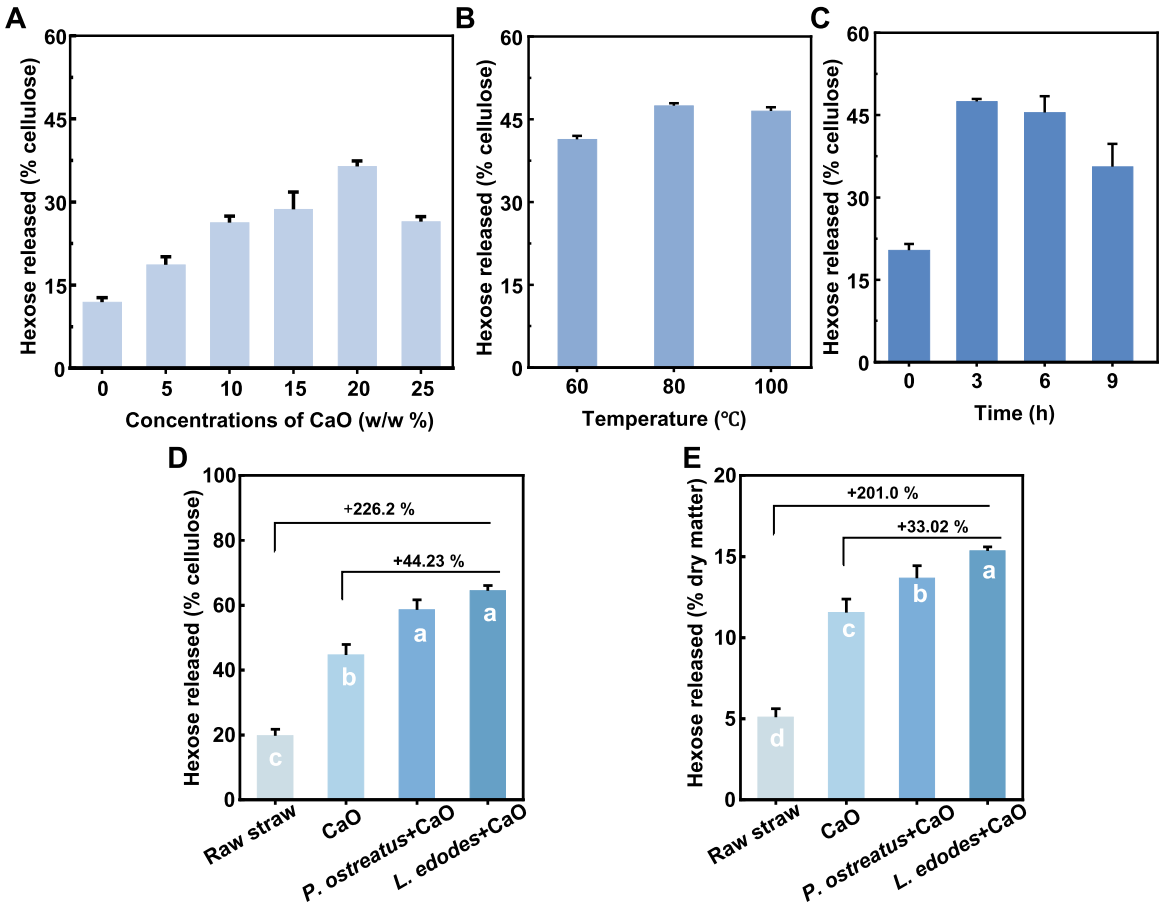

Fig. 3. Biomass saccharification by calculating hexoses yields released from enzymatic hydrolyses after optimal CaO pretreatments with the desired *Miscanthus* (Msa6) lignocellulose pre-incubated with two fungi (*P. ostreatus*, *L. edodes*) strains for 21 days. (A) CaO pretreatment with raw straw of *Miscanthus* at different concentrations; (B) 20% CaO pretreatment at different temperatures; (C) 20% CaO pretreatment at 80 ℃ under different treatment times; (D, E) Optimal CaO pretreatment (20% CaO at 80 ℃ for 3 h) with fungi pre-incubated lignocellulose; CaO as optimal pretreatment with raw straw; Bars as means ± SD (n = 3); Different letters (a-c) of the bars as significant differences among treatments ($p < 0.05$) by multiple *t*-test.

3.4. Synergistically enhanced saccharification from integrated CaO and fungi pretreatments

Since fungal incubations only extracted small amounts of hemicellulose and lignin, the second-step chemical pretreatments are conducted for further reducing lignocellulose recalcitrance. By using two recyclable solid and liquid alkali chemicals (CaO, $NH_3{\cdot}H_2O$) under a series of concentrations, this study initially attempted to find out the optimal pretreatments with raw straws of two *Miscanthus* accessions (Fig. S6) (Liu et al., 2021; Wang et al., 2025). Under 20% CaO pretreatments, two *Miscanthus* accessions showed the highest hexose yields released from enzymatic hydrolyses of pretreated-lignocellulose substrates, which were accountable distinct biomass enzymatic saccharification of two accessions. By comparison, two *Miscanthus* accessions had slightly enhanced biomass saccharification as the $NH_3{\cdot}H_2O$ concentrations were rising, but they remained much lower hexose yields than those of the CaO pretreatments. Therefore, this study focused to optimize the CaO pretreatment with desirable *Miscanthus* accession (Msa6) under various pretreatment temperatures and times (Fig. 3 A-C). The optimal CaO pretreatment (20%, 80 °C, 3 h) was further performed with the lignocellulose residues from two fungal incubations, and significantly increased hexoses yields (% cellulose or % dry matter) were determined compared to the controls (raw *Miscanthus* straw, CaO-pretreated lignocellulose) (Fig. 3 D & E), indicating a synergistic enhancement of biomass enzymatic saccharification from two-step pretreatment (fungi biological and CaO pretreatments), namely as *P. ostreatus*+CaO and *L. edodes*+CaO samples. Particularly, the *L. edodes*+CaO sample exhibited the highest hexose yields among all samples examined, which were higher than those of the control (CaO pretreatment) by 44% and 33%. suggesting a relatively more reduced lignocellulose recalcitrance from those integrated biomass processes.

3.5. Contrastively improved bioethanol and lactic acid conversions

By collecting all hexoses released from enzymatic hydrolyses, this study respectively conducted yeast (*Saccharomyces cerevisiae*) and bacterial (*Lactobacillus paracasei*) fermentations for bioethanol and lactic acid production (Fig. 4 A & B). Compared to the raw straw sample, the optimal CaO pretreatment could cause much increased bioethanol and lactic acid yields up to 3-fold, but optimal CaO pretreatments with fungal-incubated lignocelluloses further increased both bioethanol and lactic acid yields, being consistent with its enhanced biomass saccharification examined. Unexpectedly, despite that the two-step *L. edodes*+CaO pretreatments caused the highest hexoses yields, the highest bioethanol and lactic acid yields were achieved with the *P. ostreatus*+CaO sample, which were significantly higher than those of either CaO pretreatment (with raw straw) by 40% and 41% or the raw straw (without pretreatment) by 3.4- and 3.6 folds. These findings were confirmed by calculations of hexoses-ethanol and hexose-lactic acid conversion rates or by the mass balance analyses from yeast and

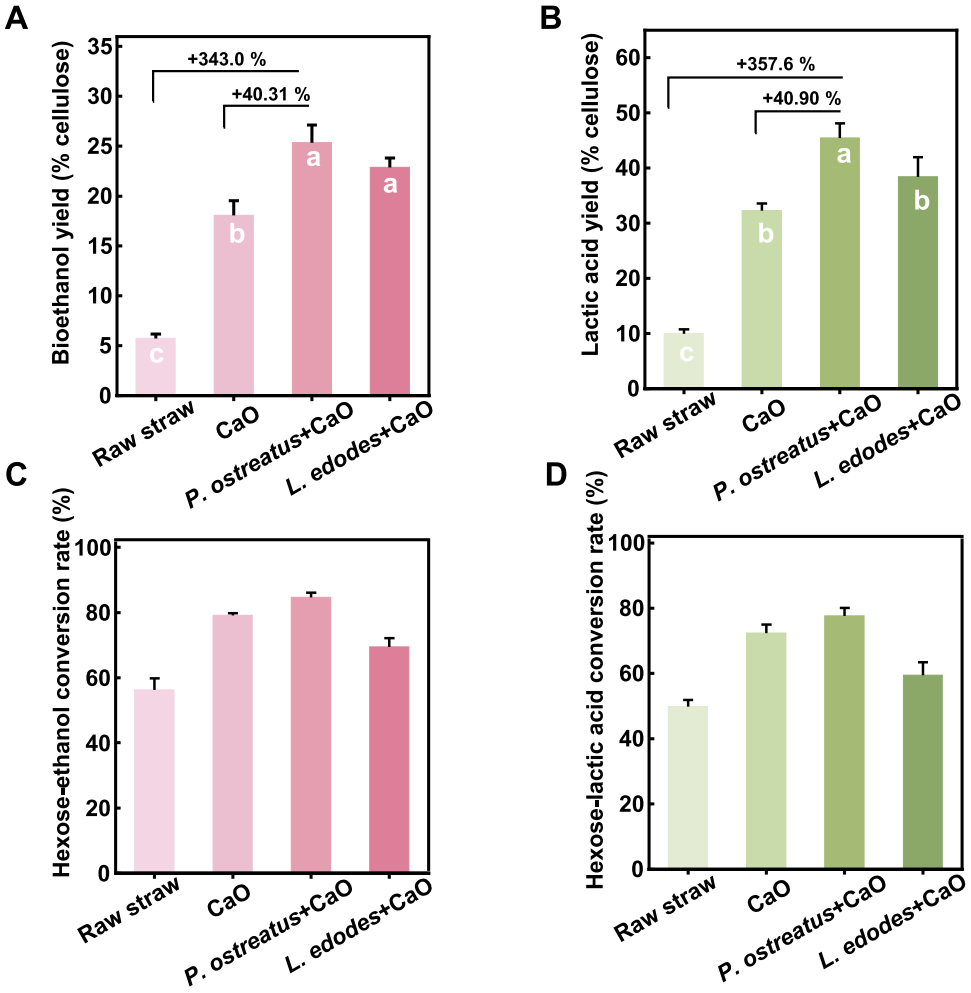

Fig. 4. Bioethanol and lactic acid productions from yeast and *L. paracasei* fermentations with the hexoses released from enzymatic hydrolyses after optimal CaO pretreatments with the desired *Miscanthus* (Msa6) straw pre-incubated with two fungi (*P. ostreatus, L. edodes*) strains for 21 days. (A) Ethanol yield (% cellulose); (B) Lactic acid yield (% cellulose). (C) Hexose-ethanol conversion rate (%). (D) Hexose-lactic acid conversion rate (%). CaO as optimal pretreatment with raw straw; Bar as means ± SD (n = 3); Different letters (a-c) of the bars as significant differences among treatments ($p < 0.05$) by multiple *t*-test.

bacterial fermentations (Fig. 4 C & D; Fig. S7), suggesting that the *P. ostreatus* incubation may produce relatively less toxic compounds that inhibit both yeast and bacterial fermentations (Gashaw et al., 2020; Giacon et al., 2025; Guido et al., 2023; Yin et al., 2025). Therefore, these two fungal incubations with desirable *Miscanthus* straw provided the selectivity for maximizing hexoses, bioethanol and lactic acid products.

3.6. Characteristic lignocellulose modifications from integrative fungal and CaO pretreatments

To understand how the lignocellulose substrates are digestible and convertible from integrative fungal and CaO pretreatments, this study observed lignocellulose morphogenesis from sequential de-lignocellulose processes of desirable *Miscanthus* (Mas6) straw (Fig. 5 A-D). Compared to the smooth and compact lignocellulose face of raw straw, the CaO-pretreated lignocellulose exhibited a rough and disrupted surface, and the integrated fungi+CaO pretreatments could further destruct lignocellulose into fragments. Particularly, the *L. edodes*+CaO sample showed the mostly disrupted lignocellulose surface, which was accountable for its relatively more lignin and hemicellulose extraction (Fig. S7). Meanwhile, this study performed a classic BET assay to detect biomass porosity in the pretreated-lignocellulose substrates (Fig. 5 E & F). Compared to the CaO-pretreated lignocellulose, both *P. ostreatus*+CaO and *L. edodes*+CaO samples respectively showed the specific surface areas raised by 58.8% and 46.5%, but only *L. edodes*+CaO sample had increased pore volume by 44.1%, being consistent with its mostly altered lignocellulose morphogenesis as just observed (Zhang et al., 2025). Based on lignocellulose crystallinity assay, all three pretreated samples showed increased CrI values relative to the raw straw (Fig. 5 G), which was mainly due to the hydrogen bonds disassociation vis wall polymer extractions by pretreatment (Alam et al., 2020). However, the *P. ostreatus*+CaO and *L. edodes*+CaO samples had relatively reduced CrI values compared to the CaO-pretreated one, which may be due to relatively more cellulose digestion from the integrated pretreatments conducted (Fig. S7). In addition, the FTIR profiling was observed for insight into interlinkage change from wall polymer extraction (Fig. S8). As a comparison with raw straw sample, the characteristic peaks associated with lignin (1241 cm^{-1}, 1512 cm^{-1}, and 1735 cm^{-1}) and hemicellulose (1053 cm^{-1}) interlinkage were altered in the pretreated samples, being accountable for effective wall polymer extraction (Ong et al., 2020; Sun et al., 2015; Zhou et al., 2017). The cellulose-associated peak at 1108 cm^{-1} was also altered in both *P. ostreatus*+CaO and *L. edodes*+CaO samples, which should be owing to more cellulose digestion for improved accessibility (Ong et al., 2020; Wittner et al., 2023; Zhang et al., 2023b).

3.7. Mechanisms of integrative depolymerization for maximum hexose, bioethanol and lactic acid production

Based on all findings achieved, this study proposed a mechanism model to explain how the fungal and CaO pretreatments were effectively integrated as the typically synergistic lignocellulose depolymerization and modification selective for maximizing hexoses, bioethanol and lactic acid production (Fig. 6). (1) Two fungal incubations with desirable *Miscanthus* straw could distinctively induce the secretions of four types of lignocellulose-degradation enzymes and cofactors, which enabled an efficient lignocellulose degradation and extraction. (2) The *L. edodes* incubation specifically secreted the manganese peroxidase at extremely high activity along with a radical-mediated oxidation pathway for an effective co-extraction of wall polymers via a dominated lignin-network deconstruction, whereas the *P. ostreatus* incubation produced relatively high-activity laccase coupled with a direct lignocellulose destruction for more cellulose digestion. (3) While the optimal CaO pretreatments were further conducted with fungal-incubated residues, the *L. edodes*+CaO pretreatment was effective for more wall polymer extraction than the *P. ostreatus*+CaO did, mainly due to distinct lignocellulose-degradation enzymes secretion and different metabolism pathways involvement. (4) Given the optimal CaO pretreatment with raw straw could largely extract lignin and hemicellulose, it caused much less cellulose digestion than the integrated fungi+CaO pretreatments did, which should be

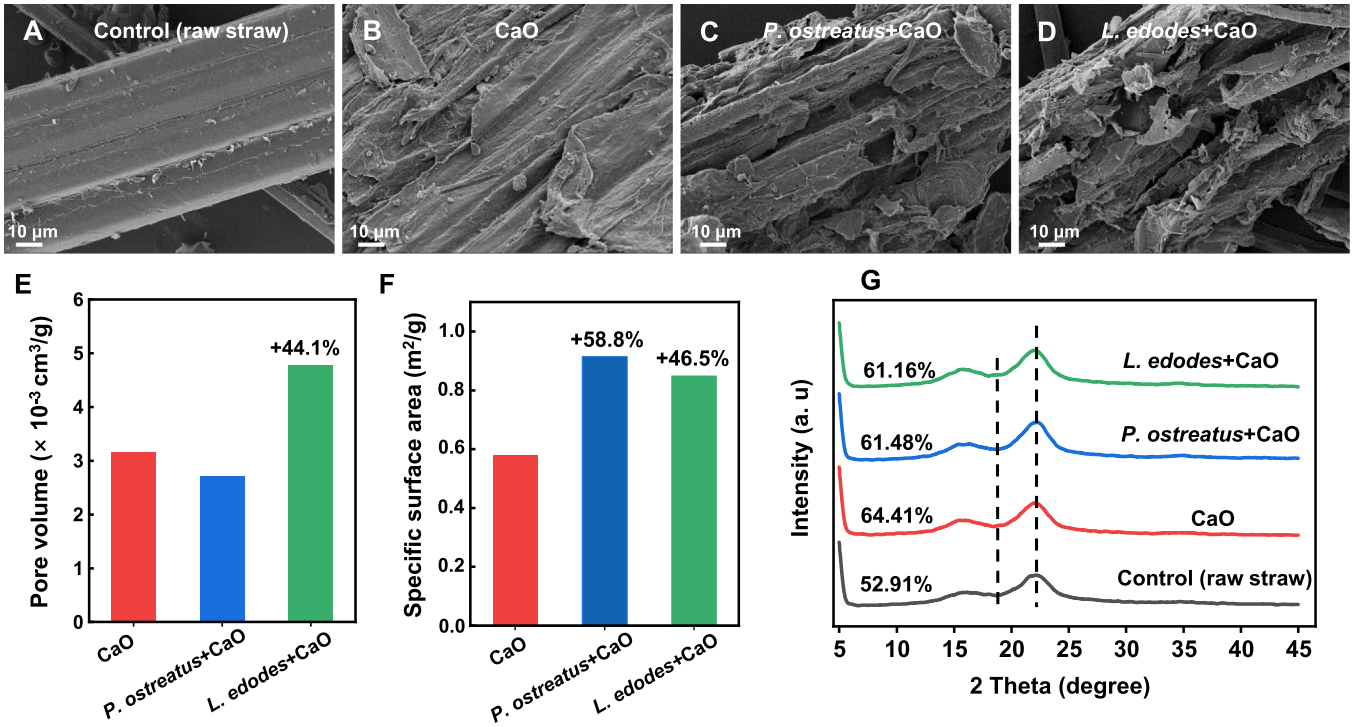

Fig. 5. Characterization of lignocellulose residues after optimal CaO pretreatments with the desired *Miscanthus* (Msa6) straw pre-incubated with two fungi (*P. ostreatus*, *L. edodes*) strains for 21 days. (A-D) SEM images of raw straw (A), 20% CaO pretreated residue (B), *P. ostreatus*+CaO pretreated residue (C), and *L. edodes*+CaO pretreated residue (D). (E, F) BET assay of pore volume specific surface area; (G) XRD profiling.

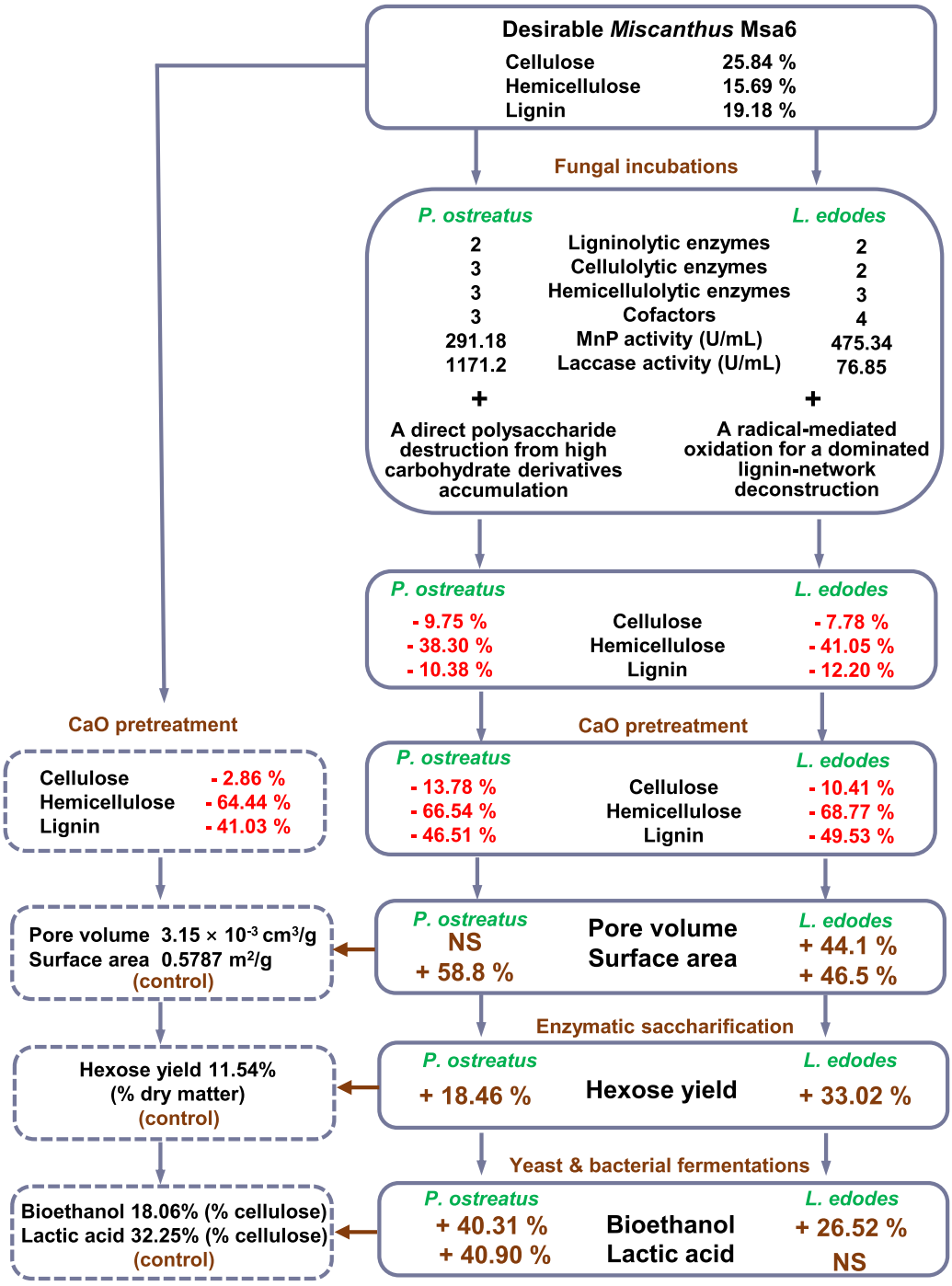

Fig. 6. A mechanism model of two fungal incubations with desirable *Miscanthus* (Msa6) straw for secretions of lignocellulose-degradation enzymes with distinctive enzyme activities and different metabolisms for integrative lignocellulose depolymerization and modification with the optimal CaO pretreatment towards synergistic enhancement of biomass saccharification and distinct bioethanol and lactic acid conversions. -% in red as reduced rate during sequential de-lignocellulose processes, and + % as increased rate relative to the control without fungal incubation; NS as non-significant different data from the control.

accountable for reduced lignocellulose porosity such as specific surface area and pore volume (Zhang et al., 2025). (5) As lignocellulose porosity is the key parameter accounting for biomass enzymatic saccharification (Zhang et al., 2023a), this model thus explained why the *L. edodes*+CaO pretreatments could achieve the highest hexose yield, due to much raised specific surface area and pore volume. (6) Even though *P. ostreatus*+CaO pretreatments had lower hexose yield than the *L. edodes*+CaO did, it achieved significantly higher bioethanol and lactic acid conversions, which suggested relatively less inhibitory compounds released from *P. ostreatus* incubation. On the other hand, it remains to explore how quantitative measurements of cellulolytic and hemicellulolytic enzyme activities could further validate the proposed hydrolytic mechanism in *P. ostreatus* in future studies, and why the *L. edodes* incubation could cause more toxic compounds that inhibit both yeast and bacterial fermentations in the future (Petraglia et al., 2025; Yin et al., 2025). Because the hexose is the universal substrate convertible for biofuels, biochemicals and bioproducts, therefore, this model has provided the optional fungal incubations selective for

maximizing hexose, bioethanol and lactic acid products.

4. Conclusions

By employing the desirable *Miscanthus* (Msa6) straw with reduced lignocellulose recalcitrance, this study demonstrates that two fungal (*P. ostreatus*, *L edodes*) incubations distinctively extract wall polymers by effective secretions of four major types of lignocellulose-degradation enzymes and cofactors along with different metabolic pathways. The integrative *L. edodes* and CaO pretreatments could further modify lignocellulose morphogenesis accountable for much raised biomass porosity such as specific surface area and pore volume, leading to a typically synergistic enhancement of biomass saccharification for the mostly increased hexose yield by 33%. By comparison, the integrated *P. ostreatus* and CaO pretreatments enable much higher bioethanol and lactic acid conversions, probably due to less toxic compounds release that inhibit yeast and bacterial fermentations. Therefore, a mechanism model has been proposed to highlight how two green-like pretreatments are effectively integrated for synergistic lignocellulose depolymerization and modification, providing a novel strategy selective to achieve maximus hexoses, bioethanol and lactic acid production.

CRediT authorship contribution statement

Hao Peng: Methodology, Investigation, Formal analysis. **Ruilan Yang:** Methodology, Investigation, Formal analysis. **Yanting Wang:** Validation, Supervision, Funding acquisition. **Peng Liu:** Validation, Supervision, Funding acquisition. **Heng Kang:** Writing – review & editing, Supervision, Methodology, Conceptualization. **Jiamin Li:** Writing – original draft, Methodology, Investigation, Formal analysis. **Liangcai Peng:** Validation, Supervision, Funding acquisition. **Yasi Zhou:** Methodology, Investigation, Formal analysis. **Yixiang Wang:** Investigation, Formal analysis. **Siqin Tan:** Methodology, Investigation, Formal analysis. **Qian Zhang:** Methodology, Investigation, Formal analysis. **Jiale Liu:** Methodology, Investigation, Formal analysis.

Declaration of Competing Interest

The authors declare no competing interests.

Acknowledgments

This work was in partial supported by the National Natural Science Foundation of China (32470273, 32570317, 32170268), Hubei Provincial Natural Science Foundation of China for Excellent Young Scientists (2024AFA100), and the Initiative Grant of Hubei University of Technology for High-level Talents (GCC20230001).

Additional information

All data are present in the paper and/or the Supplementary Materials. Additional data related to this paper may be requested from the corresponding authors.

Appendix A. Supporting information

Supplementary data associated with this article can be found in the online version at doi:10.1016/j.indcrop.2026.123224.

Data availability

Data will be made available on request.

References

Ai, Y., Wang, H., Liu, P., Yu, H., Sun, M., Zhang, R., Tang, J., Wang, Y., Feng, S., Peng, L., 2024. Insights into contrastive cellulose nanofibrils assembly and nanocrystals catalysis from dual regulations of plant cell walls. Sci. Bull. 69 (24), 3815–3819. https://doi.org/10.1016/j.scib.2024.06.013.

Alam, A., Wang, Y., Liu, F., Kang, H., Tang, S.-w, Wang, Y., Cai, Q., Wang, H., Peng, H., Li, Q., Zeng, Y., Tu, Y., Xia, T., Peng, L., 2020. Modeling of optimal green liquor pretreatment for enhanced biomass saccharification and delignification by distinct alteration of wall polymer features and biomass porosity in *Miscanthus*. Renew. Energy 159, 1128–1138. https://doi.org/10.1016/j.renene.2020.06.013.

Alam, A., Zhang, R., Liu, P., Huang, J., Wang, Y., Hu, Z., Madadi, M., Sun, D., Hu, R., Ragauskas, A.J., Tu, Y., Peng, L., 2019. A finalized determinant for complete lignocellulose enzymatic saccharification potential to maximize bioethanol production in bioenergy *Miscanthus*. Biotechnol. Biofuels 12 (1). https://doi.org/10.1186/s13068-019-1437-4.

Baksi, S., Ball, A.K., Sarkar, U., Banerjee, D., Wentzel, A., Preisig, H.A., Kuniyal, J.C., Birgen, C., Saha, S., Wittgens, B., Markussen, S., 2019. Efficacy of a novel sequential enzymatic hydrolysis of lignocellulosic biomass and inhibition characteristics of monosugars. Int. J. Biol. Macromol. 129, 634–644. https://doi.org/10.1016/j.ijbiomac.2019.01.188.

Beluhan, S., Mihajlovski, K., Šantek, B., Ivančić Šantek, M., 2023. The production of bioethanol from lignocellulosic biomass: pretreatment methods, fermentation, and downstream processing. Energies 16 (19). https://doi.org/10.3390/en16197003.

Brischke, C., Hanske, M., 2016. Durability of untreated and thermally modified reed (*Phragmites australis*) against brown, white and soft rot causing fungi. Ind. Crops Prod. 91, 49–55. https://doi.org/10.1016/j.indcrop.2016.06.031.

Chen, S., Davaritouchaee, M., 2023. Nature-inspired pretreatment of lignocellulose - Perspective and development. Bioresour. Technol. 369, 128456. https://doi.org/10.1016/j.biortech.2022.128456.

Cheng, L., Wang, L., Wei, L., Wu, Y., Alam, A., Xu, C., Wang, Y., Tu, Y., Peng, L., Xia, T., 2019. Combined mild chemical pretreatments for complete cadmium release and cellulosic ethanol co-production distinctive in wheat mutant straw. Green. Chem. 21 (13), 3693–3700. https://doi.org/10.1039/C9GC00686A.

Civzele, A., Stipniece-Jekimova, A.A., Mezule, L., 2023. Fungal ligninolytic enzymes and their application in biomass lignin pretreatment. J. Fungi 9 (7). https://doi.org/10.3390/jof9070780.

da Costa, R.M.F., Pattathil, S., Avci, U., Winters, A., Hahn, M.G., Bosch, M., 2019. Desirable plant cell wall traits for higher-quality *miscanthus* lignocellulosic biomass. Biotechnol. Biofuels 12 (1). https://doi.org/10.1186/s13068-019-1426-7.

de Cassia Spacki, K., Novi, D.M.P., de Oliveira-Junior, V.A., Durigon, D.C., Fraga, F.C., Dos Santos, L.F.O., Helm, C.V., de Lima, E.A., Peralta, R.A., de Fatima Peralta Muniz Moreira, R., Correa, R.C.G., Bracht, A., Peralta, R.M., 2023. Improving enzymatic saccharification of Peach palm (*Bactris gasipaes*) wastes via biological pretreatment with *Pleurotus ostreatus*. Plants (Basel) 12 (15). https://doi.org/10.3390/plants12152824.

de Figueiredo, F.L., de Oliveira, A.C.P., Terrasan, C.R.F., Goncalves, T.A., Gerhardt, J.A., Tomazetto, G., Persinoti, G.F., Rubio, M.V., Pena, J.A.T., Araujo, M.F., de Carvalho Silvello, M.A., Franco, T.T., Rabelo, S.C., Goldbeck, R., Squina, F.M., Damasio, A., 2021. Multi-omics analysis provides insights into lignocellulosic biomass degradation by *Laetiporus sulphureus* ATCC 52600. Biotechnol. Biofuels 14 (1), 96. https://doi.org/10.1186/s13068-021-01945-7.

Derba-Maceluch, M., García Romañach, L., Hedenström, M., Mitra, M., Donev, E.N., Urbancsok, J., Yassin, Z., Gandla, M.L., Sivan, P., Šimura, J., Scheepers, G., Jönsson, L.J., Vilaplana, F., Mellerowicz, E.J., 2025. Glucuronoyl esterase expressed in aspen xylem affects γ-ester linkages between lignin and glucuronoxylan reducing recalcitrance and accelerating growth. Plant Biotechnol. J. 23 (12), 5417–5434. https://doi.org/10.1111/pbi.70301.

Deswal, D., Gupta, R., Nandal, P., Kuhad, R.C., 2014. Fungal pretreatment improves amenability of lignocellulosic material for its saccharification to sugars. Carbohydr. Polym. 99, 264–269. https://doi.org/10.1016/j.carbpol.2013.08.045.

Ding, C., Wang, X., Li, M., 2019. Evaluation of six white-rot fungal pretreatments on corn stover for the production of cellulolytic and ligninolytic enzymes, reducing sugars, and ethanol. Appl. Microbiol Biotechnol. 103 (14), 5641–5652. https://doi.org/10.1007/s00253-019-09884-y.

Fan, X., Khanna, M., Lee, Y., Kent, J., Shi, R., Guest, J.S., Lee, D., 2024. Spatially varying costs of GHG abatement with alternative cellulosic feedstocks for sustainable aviation fuels. ES&T 58 (26), 11352–11362. https://doi.org/10.1021/acs.est.4c01949.

Gashaw, G., Fassil, A., Redi, F., 2020. Evaluation of the antibacterial activity of *Pleurotus* spp. cultivated on different agricultural wastes in chiro, Ethiopia. Int. J. Microbiol 2020, 1–9. https://doi.org/10.1155/2020/9312489.

Giacon, T.G., Vilela, N., Trivellin, C., Basso, T.O., Olsson, L., 2025. Lignocellulosic hydrolysate composition influences contamination profiles in ethanol production. Bioresour. Technol. 435. https://doi.org/10.1016/j.biortech.2025.132838.

Guido, D., Luca, C., Simone, P., Milena, M., Marcella, B., Candida, V., 2023. Proteomic characterization of Shiitake (*Lentinula edodes*) post-harvest fruit bodies grown on hardwood logs and isolation of an antibacterial serine protease inhibitor. Fungal Biol. 127 (1), 881–890. https://doi.org/10.1016/j.funbio.2022.11.004.

He, B., Hao, B., Yu, H., Tu, F., Wei, X., Xiong, K., Zeng, Y., Zeng, H., Liu, P., Tu, Y., Wang, Y., Kang, H., Peng, L., Xia, T., 2022. Double integrating XYL2 into engineered *Saccharomyces cerevisiae* strains for consistently enhanced bioethanol production by effective xylose and hexose co-consumption of steam-exploded lignocellulose in bioenergy crops. Renew. Energy 186, 341–349. https://doi.org/10.1016/j.renene.2021.12.103.

He, M., Peng, Q., Xu, X., Shi, B., Qiao, Y., 2024. Antioxidant capacities and non-volatile metabolites changes after solid-state fermentation of soybean using oyster mushroom (*Pleurotus ostreatus*) mycelium. Front. Nutr. 11, 2024. https://doi.org/10.3389/fnut.2024.1509341.

Hermosilla, E., Rubilar, O., Schalchli, H., da Silva, A.S.A., Ferreira-Leitao, V., Diez, M.C., 2018. Sequential white-rot and brown-rot fungal pretreatment of wheat straw as a promising alternative for comple mentary mild treatments. Waste Manag 79, 240–250. https://doi.org/10.1016/j.wasman.2018.07.044.

Hřebečková, T., Wiesnerová, L., Hanč, A., 2020. Change in agrochemical and biochemical parameters during the laboratory vermicomposting of spent mushroom substrate after cultivation of *Pleurotus ostreatus*. Sci. Total Environ. 739, 140085. https://doi.org/10.1016/j.scitotenv.2020.140085.

Hu, M., Yuan, L., Cai, Z., Zhang, J., Ji, D., Zang, L., 2021. Ammonia fiber expansion combined with white rot fungi to treat lignocellulose for cultivation of mushrooms. ACS Omega 6 (47), 31689–31698. https://doi.org/10.1021/acsomega.1c04388.

Huang, X., Zhang, R., Yang, Q., Li, X., Xiang, Q., 2022. Cultivating *Lentinula edodes* on substrate containing composted sawdust affects the expression of car. mSystems 7, e00827–00821. https://doi.org/10.1128/msystems.00827-21.

Kapich, A.N., Korneichik, T.V., Hatakka, A., Hammel, K.E., 2010. Oxidizability of unsaturated fatty acids and of a non-phenolic lignin structure in the manganese peroxidase-dependent lipid peroxidation system. Enzym. Microb. Technol. 46 (2), 136–140. https://doi.org/10.1016/j.enzmictec.2009.09.014.

Kipping, L., Jehmlich, N., Moll, J., Noll, M., Gossner, M.M., Van Den Bossche, T., Edelmann, P., Borken, W., Hofrichter, M., Kellner, H., 2024. Enzymatic machinery of wood-inhabiting fungi that degrade temperate tree species. ISME J. 18 (1). https://doi.org/10.1093/ismejo/wrae050.

Li, Y., Liu, P., Huang, J., Zhang, R., Hu, Z., Feng, S., Wang, Y., Wang, L., Xia, T., Peng, L., 2018. Mild chemical pretreatments are sufficient for bioethanol production in transgenic rice straws overproducing glucosidase. Green. Chem. 20 (9), 2047–2056. https://doi.org/10.1039/C8GC00694F.

Li, F., Liu, Y., Jia, J., Yu, H., 2023. Combination of biological pretreatment with deep eutectic solvent pretreatment for enhanced enzymatic saccharification of Pinus massoniana. Bioresour. Technol. 380, 129110. https://doi.org/10.1016/j.biortech.2023.129110.

Li, T., Peng, H., He, B., Hu, C., Zhang, H., Li, Y., Yang, Y., Wang, Y., Bakr, M.M.A., Zhou, M., Peng, L., Kang, H., 2024. Cellulose de-polymerization is selective for bioethanol refinery and multi-functional biochar assembly using brittle stalk of corn mutant. Int. J. Biol. Macromol. 264. https://doi.org/10.1016/j.ijbiomac.2024.130448.

Li, M., Si, S., Hao, B., Zha, Y., Wan, C., Hong, S., Kang, Y., Jia, J., Zhang, J., Li, M., Zhao, C., Tu, Y., Zhou, S., Peng, L., 2014. Mild alkali-pretreatment effectively extracts guaiacyl-rich lignin for high lignocellulose digestibility coupled with largely diminishing yeast fermentation inhibitors in *Miscanthus*. Bioresour. Technol. 169, 447–454. https://doi.org/10.1016/j.biortech.2014.07.017.

Liu, F., Li, J., Yu, H., Li, Y., Wang, Y., Gao, H., Peng, H., Hu, Z., Wang, H., Zhang, G., Tu, Y., Peng, L., 2021. Optimizing two green-like biomass pretreatments for maximum bioethanol production using banana pseudostem by effectively enhancing cellulose depolymerization and accessibility. Sust. Energy Fuels 5 (13), 3467–3478. https://doi.org/10.1039/d1se00613d.

Liu, P., Wang, Y., Kang, H., Wang, Y., Yu, H., Peng, H., He, B., Xu, C., Jia, K.-Z., Liu, S., Xia, T., Peng, L., 2024. Upgraded cellulose and xylan digestions for synergistic enhancements of biomass enzymatic saccharification and bioethanol conversion using engineered *Trichoderma reesei* strains overproducing mushroom LeGH7 enzyme. Int. J. Biol. Macromol. 278. https://doi.org/10.1016/j.ijbiomac.2024.134524.

Meenakshisundaram, S., Fayeulle, A., Leonard, E., Ceballos, C., Pauss, A., 2021. Fiber degradation and carbohydrate production by combined biological and chemical/physicochemical pretreatment methods of lignocellulosic biomass - A review. Bioresour. Technol. 331, 125053. https://doi.org/10.1016/j.biortech.2021.125053.

Monteiro, L.M.O., del Cerro, C., Kijpornyongpan, T., Yaguchi, A., Bennett, A., Donohoe, B.S., Ramirez, K.J., Benson, A.F., Mitchell, H.D., Purvine, S.O., Markillie, L.M., Burnet, M.C., Bloodsworth, K.J., Bowen, B.P., Harwood, T.V., Louie, K., Northen, T., Salvachúa, D., 2025. Metabolic profiling of two white-rot fungi during 4-hydroxybenzoate conversion reveals biotechnologically relevant biosynthetic pathways. Commun. Biol. 8 (1). https://doi.org/10.1038/s42003-025-07640-9.

Nguyen, T.V.T., Gye, H., Baek, H., Han, S., Kim, Y.H., 2024. Selective adsorption of lignin peroxidase on lignin for biocatalytic conversion of poplar wood biomass to value-added chemicals. ACS Appl. Mater. Interfaces 16 (45), 62203–62212. https://doi.org/10.1021/acsami.4c14971.

Ong, H.C., Chen, W.-H., Singh, Y., Gan, Y.Y., Chen, C.-Y., Show, P.L., 2020. A state-of-the-art review on thermochemical conversion of biomass for biofuel production: a TG-FTIR approach. Energy Convers. Manag. 209. https://doi.org/10.1016/j.enconman.2020.112634.

Paz Cedeno, F.R., Petrielli, G.P., Medeiros, S.R. d, Berndt, A., Hernandes, T.A.D., Bonomi, A., Driemeier, C., 2025. Biorefining lignocellulose into feed and food: the case of sugarcane and a technology outlook. Front. Bioeng. Biotechnol. 13. https://doi.org/10.3389/fbioe.2025.1653367.

Pei, Y., Li, Y., Zhang, Y., Yu, C., Fu, T., Zou, J., Tu, Y., Peng, L., Chen, P., 2016. G-lignin and hemicellulosic monosaccharides distinctively affect biomass digestibility in rapeseed. Bioresour. Technol. 203, 325–333. https://doi.org/10.1016/j.biortech.2015.12.072.

Pellegrino, R.M., Blasi, F., Angelini, P., Ianni, F., Alabed, H.B.R., Emiliani, C., Venanzoni, R., Cossignani, L., 2022. LC/MS Q-TOF metabolomic investigation of amino acids and dipeptides in *Pleurotus ostreatus* grown on different substrates. J. Agric. Food Chem. 70 (33), 10371–10382. https://doi.org/10.1021/acs.jafc.2c04197.

Peng, L., Hocart, C.H., Redmond, J.W., Williamson, R.E., 2000. Fractionation of carbohydrates in arabidopsis root cell walls shows that three radial swelling loci. Planta 211 (3), 406–414. https://doi.org/10.1007/s004250000301.

Petraglia, T., Latronico, T., Liuzzi, G.M., Fanigliulo, A., Crescenzi, A., Rossano, R., 2025. Hydrolytic enzymes in the secretome of the mushrooms *P. eryngii* and *P. ostreatus*: a comparison between the two species. Molecules 30 (12), 2505. https://doi.org/10.3390/molecules30122505.

Pinar, O., Rodríguez-Couto, S., 2024. Biologically active secondary metabolites from white-rot fungi. Front. Chem. 12, 2024. https://doi.org/10.3389/fchem.2024.1363354.

Qi, S., Martín, C., Xiong, S., Xie, J., Chen, F., 2025. Fungal pretreatment of hardwood for cellulosic ethanol production: Formation of by-products and the potential effects on downstream bioconversion processes. Ind. Crops Prod. 237, 122270. https://doi.org/10.1016/j.indcrop.2025.122270.

Qi, J., Zhang, X., Zhou, Y., Zhang, C., Wen, J., Deng, S., Luo, B., Fan, M., Xia, Y., 2023. Selectively enzymatic conversion of wood constituents with white and brown rot fungi. Ind. Crops Prod. 199, 116703. https://doi.org/10.1016/j.indcrop.2023.116703.

Saha, B.C., Qureshi, N., Kennedy, G.J., Cotta, M.A., 2016. Biological pretreatment of corn stover with white-rot fungus for improved enzymatic hydrolysis. Int. Biodeterior. Biodegrad 109, 29–35. https://doi.org/10.1016/j.ibiod.2015.12.020.

Siaperas, R., Papadaki, E., Giannikos, P., Zerva, A., Topakas, E., 2025. Genomic, proteomic, and biochemical study of *Pleurotus pulmonarius* secretome and its role in biomass saccharification. J. Agric. Food Chem. 73 (44), 28539–28551. https://doi.org/10.1021/acs.jafc.5c09170.

Skiba, E.A., Shavyrkina, N.A., Budaeva, V.V., Ovchinnikova, E.V., Mironova, G.F., Gladysheva, E.K., Zenkova, A.A., Kashcheyeva, E.I., Zolotukhin, V.N., Hong, F.F., Sakovich, G.V., 2026. Biotechnological transformation of *Miscanthus* x giganteus: technological and environmental aspects. Bioresour. Technol. 439, 133374. https://doi.org/10.1016/j.biortech.2025.133374.

Song, L., Yu, H., Ma, F., Zhang, X., 2013. Biological pretreatment under non-sterile conditions for enzymatic hydrolysis of corn stover. Bioresources 8 (3), 3802-3816. https://doi.org/10.1016/j.ibiod.2015.12.020.

Sun, S.L., Sun, S.N., Wen, J.L., Zhang, X.M., Peng, F., Sun, R.C., 2015. Assessment of integrated process based on hydrothermal and alkaline treatments for enzymatic saccharification of sweet sorghum stems. Bioresour. Technol. 175, 473–479. https://doi.org/10.1016/j.biortech.2014.10.111.

Tang, L., Shang, J., Song, C., Yang, R., Shang, X., Mao, W., Bao, D., Tan, Q., 2020. Untargeted metabolite profiling of antimicrobial compounds in the brown film of *Lentinula edodes* mycelium via LC–MS/MS analysis. ACS Omega 5 (13), 7567–7575. https://doi.org/10.1021/acsomega.0c00398.

Wan, C., Li, Y., 2012. Fungal pretreatment of lignocellulosic biomass. Biotechnol. Adv. 30, 1447–1457. https://doi.org/10.1016/j.biotechadv.2012.03.003.

Wang, H., Li, S., Wu, L., Zou, W., Zhang, M., Wang, Y., Lv, Z., Chen, P., Liu, P., Yang, Y., Peng, L., Wang, Y., 2025. Semi-overexpressed OsMYB86L2 specifically enhances cellulose biosynthesis to maximize bioethanol productivity by cascading lignocellulose depolymerization via integrated rapid-physical and recyclable-chemical processes. Green. Chem. 27 (30), 9127–9143. https://doi.org/10.1039/d5gc00658a.

Wang, M., Wang, Y., Liu, J., Yu, H., Liu, P., Yang, Y., Sun, D., Kang, H., Wang, Y., Tang, J., Fu, C., Peng, L., 2024. Integration of advanced biotechnology for green carbon. Green. Carbon 2 (2), 164–175. https://doi.org/10.1016/j.greenca.2024.02.006.

Wittner, N., Slezsak, J., Broos, W., Geerts, J., Gergely, S., Vlaeminck, S.E., Cornet, I., 2023. Rapid lignin quantification for fungal wood pretreatment by ATR-FTIR spectroscopy. Spectrochim. Acta A 285, 121912. https://doi.org/10.1016/j.saa.2022.121912.

Yin, Y., Chen, B., Xu, S., Zuo, J., Xu, Y., Xiong, S., Chen, F., 2025. Investigation of crop straw for edible and medicinal fungi cultivation: assessment of lignocellulose preprocessing and spent substrate biofuel properties. Ind. Crops Prod. 223, 120004. https://doi.org/10.1016/j.indcrop.2024.120004.

Yu, H., Zhang, G., Liu, J., Liu, P., Peng, H., Teng, Z., Li, Y., Ren, X., Fu, C., Tang, J., Li, M., Wang, Y., Wang, L., Peng, L., 2025. A functional cascading of lignin modification via repression of caffeic acid O-methyltransferase for bioproduction and anti-oxidation in rice. J. Adv. Res. 78, 1–9. https://doi.org/10.1016/j.jare.2025.01.048.

Zhang, R., Gao, H., Wang, Y., He, B., Lu, J., Zhu, W., Peng, L., Wang, Y., 2023a. Challenges and perspectives of green-like lignocellulose pretreatments selectable for low-cost biofuels and high-value bioproduction. Bioresour. Technol. 369. https://doi.org/10.1016/j.biortech.2022.128315.

Zhang, R., Hu, Z., Wang, Y., Hu, H., Li, F., Li, M., Ragauskas, A., Xia, T., Han, H., Tang, J., Yu, H., Xu, B., Peng, L., 2023b. Single-molecular insights into the breakpoint of cellulose nanofibers assembly during saccharification. Nat. Commun. 14 (1). https://doi.org/10.1038/s41467-023-36856-8.

Zhang, H., Wang, Y., Peng, H., He, B., Li, Y., Wang, H., Hu, Z., Yu, H., Wang, Y., Zhou, M., Peng, L., Wang, M., 2025. Distinct lignocelluloses of plant evolution are optimally selective for complete biomass saccharification and upgrading Cd^{2+}/Pb^{2+}

and dye adsorption via desired biosorbent assembly. Bioresour. Technol. 417. https://doi.org/10.1016/j.biortech.2024.131856.
Zhao, Y., Yao, Y., Li, H., Han, Z., Ma, X., 2024. Integrated transcriptome and metabolism unravel critical roles of carbon metabolism and oxidoreductase in mushroom with Korshinsk peashrub substrates. BMC Genom. 25 (1). https://doi.org/10.1186/s12864-024-10666-8.
Zhou, X., Li, Q., Zhang, Y., Gu, Y., 2017. Effect of hydrothermal pretreatment on *Miscanthus* anaerobic digestion. Bioresour. Technol. 224, 721–726. https://doi.org/10.1016/j.biortech.2016.10.085.